

ChemComm

Accepted Manuscript



This is an *Accepted Manuscript*, which has been through the Royal Society of Chemistry peer review process and has been accepted for publication.

Accepted Manuscripts are published online shortly after acceptance, before technical editing, formatting and proof reading. Using this free service, authors can make their results available to the community, in citable form, before we publish the edited article. We will replace this *Accepted Manuscript* with the edited and formatted *Advance Article* as soon as it is available.

You can find more information about *Accepted Manuscripts* in the [Information for Authors](#).

Please note that technical editing may introduce minor changes to the text and/or graphics, which may alter content. The journal's standard [Terms & Conditions](#) and the [Ethical guidelines](#) still apply. In no event shall the Royal Society of Chemistry be held responsible for any errors or omissions in this *Accepted Manuscript* or any consequences arising from the use of any information it contains.

COMMUNICATION

Hierarchical mesoporous yolk-shell structured carbonaceous nanospheres for high performance electrochemical capacitive energy storage

Cite this: DOI: 10.1039/x0xx00000x

Received 00th January 2012,
Accepted 00th January 2012

DOI: 10.1039/x0xx00000x

www.rsc.org/

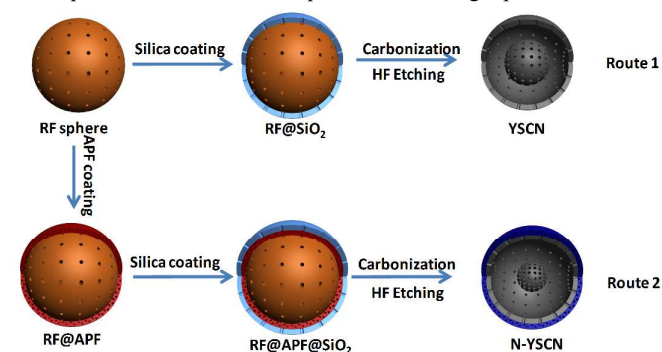
Tianyu Yang,^a Ruifeng Zhou,^{a, b} Da-Wei Wang,^c San Ping Jiang,^d Yusuke Yamauchi,^e Shi Zhang Qiao,^{b, *} Michael J. Monteiro,^{a, *} and Jian Liu^{a, d, *}

Hierarchical mesoporous yolk-shell structured carbon nanospheres (YSCNs) with ordered mesoporous carbon core and microporous carbon shell show excellent electrochemical performance with a maximal specific capacitance of 159 F·g⁻¹.

Electrochemical capacitors (ECs) (supercapacitors) are one of the energy storage devices that have been widely used in the development of hybrid vehicles.^{1, 2} Carbon materials with hierarchical porous structures were reported as the typical electrodes for improving the supercapacitor performance. For instance, the micropores (< 2 nm) can accommodate charge and strengthen capacitance, mesopores (2-50 nm) favour ion transport, and macropores (> 50 nm) allow ion-buffering.³ Until now, great efforts have been devoted to synthesising hierarchical porous carbons; however, in most cases, the pore size is randomly distributed in the bulk material.^{4, 5} It is still a challenge to synthesise hierarchical porous carbon with different pore size in a controlled sequence. This hierarchical structure will provide an opportunity to understand the role of different scaled pores and guide in the design of high rate devices. The recent development of yolk-shell structures provides an ideal synthetic strategy to produce such hierarchical porous carbon.⁶⁻⁹ To the best of our knowledge, there are no reports on the hierarchical porous yolk-shell structured carbon spheres, in particularly, with mesoporous carbon core and microporous carbon shell.

In the last ten years, the nanoporous carbonaceous spheres with diverse nanostructured morphologies, such as solid, hollow, core-shell, yolk-shell have attracted great interest for promising applications in therapeutic delivery carriers, nanoreactors and energy conversion or storage.⁶⁻¹⁴ Recently, we have successfully synthesised various carbon spheres with different particle sizes, pore sizes, and structures.¹⁵⁻¹⁹ Moreover, hollow structured N-doped carbon nanocapsules with a mesoporous carbon shell and a macroporous void were prepared via an outer silica assisted method.²⁰ The versatile Stöber method for coating various carbon spheres along with our well established carbon spheres library¹⁵⁻¹⁹ allowed us to design and synthesise yolk-shell carbon nanospheres (YSCNs) with unique core@void@shell structure, namely, hierarchical porous

structure with a combination of micropores, mesopores and macropores with controlled sequence in one single particle.



Scheme 1. Schematic illustration of the procedure for synthesis of yolk-shell structured carbon nanosphere (YSCN) in route 1 and nitrogen doped yolk-shell structured carbon nanosphere (N-YSCN) in route 2.

Herein, we report a versatile Stöber coating method to synthesise YSCNs (in Route 1) and nitrogen doped yolk-shell structured carbon nanospheres (N-YSCNs, in Route 2). As shown in Scheme 1 (Route 1), the as-synthesised mesoporous resorcinol formaldehyde (RF) resin nanospheres were prepared by a dual surfactant soft template method as previously reported with a slightly modification.¹⁶ Mesoporous silica layer was then coated on the surface of as-synthesised RF nanospheres to form RF@SiO₂ core-shell nanospheres. During pyrolysis under an inert gas, the as-synthesised RF nanospheres formed carbon particles through dehydrogenation and aromatisation of the carbonisation process. The morphology transition took place with the assistance of hydrogen bonding between RF surface and silica layer. After HF etching to remove the silica layer, the mesoporous carbon core@porous carbon shell YSCNs with tailorable pore size on the shell were generated. In order to selectively dope the heteroatom nitrogen on the carbon shell of YSCN to form nitrogen doped yolk-shell carbon nanospheres (N-YSCNs), an aminophenol formaldehyde polymer layer was alternatively coated on the surface of as-synthesised RF resin nanospheres. After silica coating, carbonisation and HF etching, the

desired N-YSCNs with a nitrogen doped carbon shell can be generated as shown in Scheme 1 (Route 2). In particular, we demonstrate that both the pore size on the shell and void space between core and shell can all be well controlled by precise tuning of the synthesis parameters. To demonstrate the benefits of such hierarchical structures in energy storage, supercapacitor performance was then evaluated by using these yolk-shell structured carbons as electrodes.

As described in the experimental section, the resulting YSCNs were denoted as YSCN-*a-b*. The TEM image of YSCN-200-700 (Figure 1a) shows a very uniform yolk-shell particle with size of 190 nm, shell thickness of 21 nm, and yolk size of 60 nm in diameter. Interestingly, the yolk of YSCN-200-700 has an ordered 2D hexagonal mesoporous structure with a pore size of 8.2 nm (Figure 1b). The yolk-shell morphology has a smooth surface further confirmed by SEM (Figures 1c, d). The N₂ sorption isotherm shows a mixture of I and IV type with a steep H3 hysteresis loop, revealing a hierarchical porous structure with combined microporous, mesoporous and macroporous structure (Figure 1e). The YSCN-200-700 has a very high BET surface area (1068 m²/g) with large pore volume (0.97 cm³/g) as shown in Table 1, and around 30% surface area is calculated to be contributed by micropores. From the pore size distributions (Figure 1f), the uniform micropore size centred at 0.6 nm, mesopore size at 8.9 nm and macropore size at 72 nm are observed. These pore size distributions might be related to micropores on the shell, mesopores of yolk, and macropores of hollow spaces between yolk and shell, respectively. With increasing the carbonisation temperature, the resultant YSCN-200-900 has a higher surface area (1623 m²/g) and pore volume (1.53 cm³/g) as shown in Table 1. Moreover, the XRD pattern supports its amorphous property (Figure 1g). These results confirm that hierarchical yolk shell structured carbon spheres with a microporous (0.6 nm) shell, mesoporous (8.9 nm) core, and macroporous (~72 nm) void have been successfully fabricated.

Table 1 Textural Parameters of Porous Carbon Nanospheres^a

Sample	S _{BET} (m ² /g)	S _{micro} (m ² /g)	V _{total} (cm ³ /g)	V _{micr} (cm ³ /g)
YSCN-200-700	1068	343	0.97	0.15
YSCN-200-900	1623	551	1.53	0.24
LP-YSCN-200-900	1222	397	1.78	0.18
N50-YSCN---200-700	807	174	0.74	0.07

^a S_{BET} is specific surface area calculated from BET equation in the relative pressure range of 0.05-0.25; V_{total} is single point pore volume obtained from adsorption isotherms at P/P₀=0.99; S_{micro} and V_{micro} are specific surface area and pore volume of micropores calculated from t-plot model.

To control the void space, different shell thicknesses of silica were coated on the surface of meso-RF NPs. The silica shell thickness can be precisely adjusted from 15, 17, 22 to 26 nm (Figure S1), respectively, by simply tuning the amount of silica precursor, tetraethyl orthosilicate (TEOS), from 80, 100, 150 to 200 μL. After pyrolysis at 700 °C, it was found that solid phase separation started to occur when the silica shell is 15 nm. The thicker the silica shell, the smoother of carbon shell surface (Figures S2 a-c) and a more confined void space (Figures S2 d-f) would be obtained in the

resulting YSCNs. To further control the pore size and structures of carbon shell, as-synthesised RF NPs were soaked in an iron salt aqueous solution before coating the silica layer. The resulting YSCNs can generate large pore on the carbon shell (denoted as LP-YSCNs-*a-b*) (Figure S3).

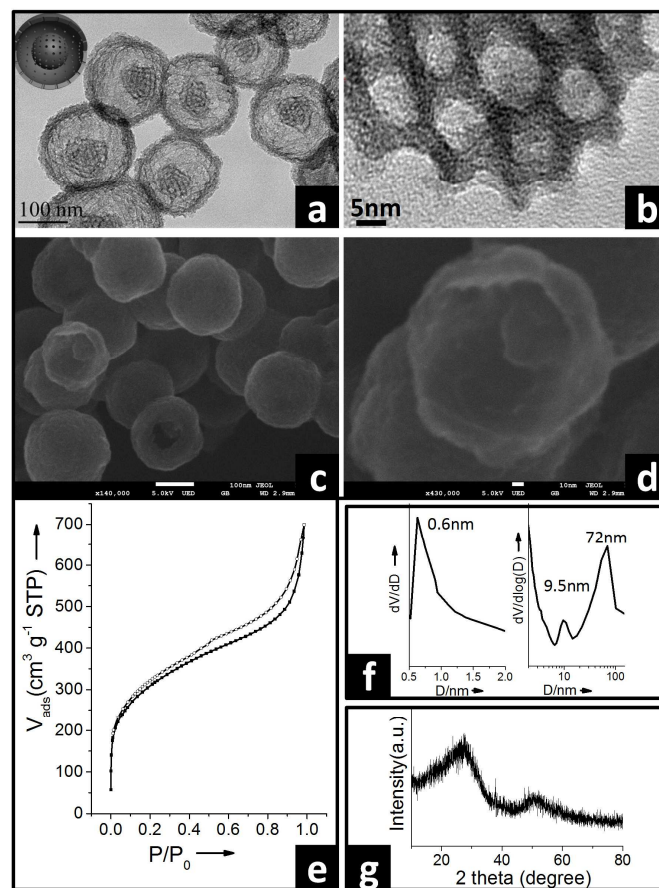


Figure 1. a) TEM image of YSCN-200-700; b) HRTEM of yolk in YSCN-200-700; c) SEM image of YSCN-200-700; d) HRSEM image of broken YSCN-200-700; e) N₂ sorption of isotherm of YSCN-200-700; f) pore size distribution of YSCN-200-700; g) XRD pattern of YSCN-200-700.

Active heteroatom nitrogen can also be selectively doped on the shell of YSCN to form nitrogen doped yolk-shell structured carbon nanospheres (N-YSCNs, Route 2). An aminophenol formaldehyde resin polymer layer was coated on the surface of as-synthesised RF NPs to obtain as-synthesised RF@APF NPs (Figure S4). This was followed by coating with silica, pyrolysis and HF etching to obtain the resulting denoted N-*m*-YSCN-*a-b* (Scheme 1). From TEM (Figure 2a), the spherical N-50-YSCN-200-700 has a uniform particle size of 196 nm with a 24 nm thick N-doped carbon shell. The HRTEM clearly shows the ordered mesoporous yolk is encapsulated into the hollow space (Figure 2b). The SEM image (Figure 2c) shows a smooth surface with uniform mesopore on the carbon shell and carbon yolk located in the hollow space of the broken hemisphere. The HRSEM image (Figure 2d) illustrates that the yolk of N-50-YSCN-200-700 has a uniform mesostructure. The mixed type I and IV N₂ sorption isotherms indicate the production of a hierarchical micro-meso porous structure. The relatively low surface area (807 m²/g) and pore volume (0.73 cm³/g) might be attributed to a thick N-doped carbon shell in which the porous channel did not fully open (Table 1). To control the N doped carbon shell thickness

and carbon yolk diameter, different amounts of carbon precursors, aminophenol, were used to precisely adjust the shell thickness and yolk size (Figures S5 and S6). It was found that the yolk size decreased from 80 to 40 nm as the N doped carbon shell thickness increased from 22 to 55 nm. Accordingly, the surface area of N-YSCNs can also be tailor from 1035 to 646 m²/g, which is due to the loss of opened porous channel on the N doped carbon shell with increased thickness (Table S1). The XPS survey spectrum shows that the surface chemistry of N-50-YSCN-200-700 shell consists of carbon, oxygen and nitrogen in the atom ratio 92.0%, 5.1% and 2.9%, respectively. The high resolution N 1s spectrum illustrates three overlapping peaks corresponding to pyridinic nitrogen (398.5 eV), graphitic nitrogen (400.6 eV) and oxidised nitrogen (401.9 eV). From the above two synthesis routes, various hierarchical porous yolk-shell carbon spheres have been synthesised, in which both the pore size on the shell and the void space can be tailored. The structure of porous carbon shell can be graphitic carbon or N-doped carbon.

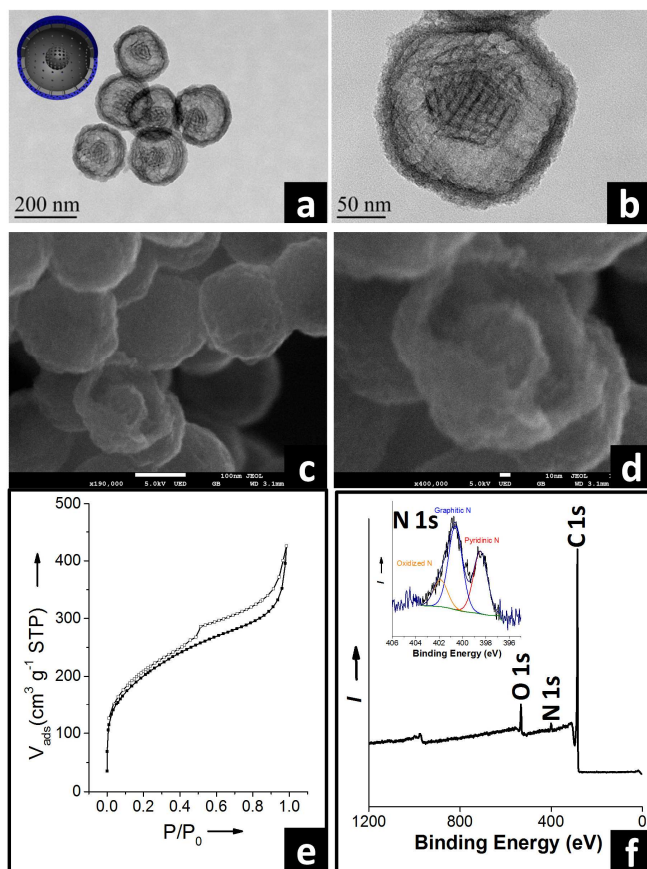


Figure 2. a) TEM image of N-50-YSCN-200-700; b) HRTEM image of N-50-YSCN-200-700; c) SEM image of N-50-YSCN-200-700; d) HRSEM image of N-50-YSCN-200-700; e) N₂ sorption isotherm of N-50-YSCN-200-700; f) XPS survey spectrum of N-50-YSCN-200-700 and its corresponding high resolution N 1s spectrum.

The supercapacitor performances of the obtained YSCNs, LP-YSCNs and N-YSCNs were measured by cyclic voltammogram (CV) and galvanostatic charge/discharge in a three-electrode system. Figures 3, S7, S8 and S9 show the CV curves of the YSCNs and N-YSCNs obtained from three-electrode cell under a potential window of -1.1 to 0.3 V (vs Ag/AgCl) at different scan rates. The specific capacities of YSCN-200-700, YSCN-200-900, N-50-YSCN-200-700, N-

200-YSCN-200-700 are 107, 139, 145, 159 F/g (in 10 mV/s), respectively. Compared with the sample pyrolysed at 700 °C (YSCN-200-700), the 900 °C pyrolysis samples (YSCN-200-900) has a relatively good rectangular shape at a voltage scan rate up to 500 mV/s (Figure 3), indicating typical double-layer capacitance behaviour and excellent high rate capacitance, which is mainly attributed from abundant micropores generated in our carbon NPs during the high temperature carbonisation process. The peaks at the end of CV scan are probably subject to the carbon oxidation during this process and could be eliminated by selecting lower potential range. In addition, large mesopores generated in LP-YSCN-200-900 shows minimum capacities reduction in high scan rate (Figure S7) due to ion-buffer effect provided by its large mesopores. Introducing active heteroatom nitrogen doped carbon shell can improve the electrochemical performance because nitrogen atoms can act as electron donor and improve the electronic conductivity of YSCNs. (Figure S8) The capacity of N-YSCN series is significantly higher than that of YSCN series, which is due to the nitrogen doping (Table S2). Graphitic nitrogen and oxidized nitrogen as shown in Figure 2f can improve the electrical conductivity of electrodes, pyridinic nitrogen is responsible for the enhanced pseudocapacitance.²¹ Moreover, N-YSCNs series have superior electronic capacitance compared to that of core-shell structured N-CSCNs (Table S2) because of the abundant mesopores and macropores in N-YSCNs, contributing to low-resisted ion diffusion and improved capacitance due to a greater ion-buffer reservoir. The charge/discharge curves of the YSCN-200-900, N-50-YSCN-200-900 and LP-YSCN-200-900 in Figure S10 a-c show the expected triangular shapes at current densities ranging from 1 to 20 A/g, indicating excellent conductivity of these yolk-shell structured nanoparticles. In Figure S10 d, the LP-YSCN-200-900 performed superior specific capacitance and slower capacitance retention than YSCN-200-900 and N50-YSCN-200-900 at a high current density 20 A/g.

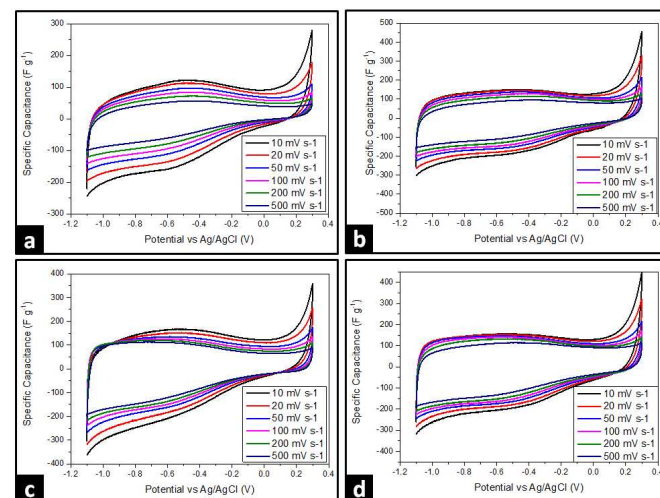


Figure 3. a-d) CV curve of YSCN-200-700, YSCN-200-900, N-50-YSCN-200-700, N-50-YSCN-200-900 respectively.

Conclusions

In conclusion, we have successfully prepared yolk-shell structured carbon nanospheres (YSCNs) with an ordered mesoporous carbon yolk and microporous carbon shell in a controlled sequence. Moreover, we have demonstrated that the pore size on the shell can be tailored from a micropore (0.6 nm)

scale to large mesopores (~40 nm), the hollow space also can be varied by tuning the thickness of the silica layer coating. Furthermore, yolk-shell carbon spheres with a graphitic carbon or N-doped carbon shell have also been designed by using aminophenol formaldehyde resin as a coating layer following with a carbonisation process. These yolk-shell carbon nanospheres have excellent performances (a maximal specific capacitance of $159 \text{ F} \cdot \text{g}^{-1}$) as supercapacitor electrodes due to their hierarchical porous structures. Abundant micropores in YSCNs result in typical double layer capacitance behaviour and excellent high rate capacitance; large mesopores in LP-YSCNs show minimum capacitance reduction in high scan rate as their ion-buffer effect; and introducing active nitrogen doped carbon shell improve the electrochemical performance because nitrogen atoms can act as electron donor. Alternatively, these hierarchical carbons would have promising applications in many fields such as drug delivery.

^a Australian Institute for Bioengineering and Nanotechnology, The University of Queensland, Brisbane, QLD 4072, Australia

^b School of Chemical Engineering, The University of Adelaide, Adelaide, SA5005, Australia

^c School of Chemical Engineering, The University of New South Wales, Sydney, NSW 2052, Australia

^d Department of Chemical Engineering, Curtin University, Perth, WA 6845, Australia

^e World Premier International (WPI) Research Center for Materials Nanoarchitectonics (MANA), National Institute for Materials Science (NIMS), 1-1 Namiki, Tsukuba, Ibaraki 305-0044, Japan

* Addresses correspondence to: jian.liu@curtin.edu.au; s.qiao@adelaide.edu.au; m.monteiro@uq.edu.au

Notes and references

1. Y. Zhai, Y. Dou, D. Zhao, P. F. Fulvio, R. T. Mayes and S. Dai, *Adv. Mater.*, 2011, **23**, 4828-4850.
2. B. Hu, K. Wang, L. Wu, S.-H. Yu, M. Antonietti and M.-M. Titirici, *Adv. Mater.*, 2010, **22**, 813-828.
3. D.-W. Wang, F. Li, M. Liu, G. Q. Lu and H.-M. Cheng, *Angew. Chem. Int. Ed.*, 2008, **47**, 373-376.
4. A.-H. Lu, G.-P. Hao, Q. Sun, X.-Q. Zhang and W.-C. Li, *Macromol. Chem. Phys.*, 2012, **213**, 1107-1131.
5. J. Tang, J. Liu, N. L. Torad, T. Kimura and Y. Yamauchi, *Nano Today*, 2014, **9**, 305-323.
6. Y. Chen, P. Xu, M. Wu, Q. Meng, H. Chen, Z. Shu, J. Wang, L. Zhang, Y. Li and J. Shi, *Adv. Mater.*, 2014, **26**, 4294-4301.
7. Y. Fang, D. Gu, Y. Zou, Z. Wu, F. Li, R. Che, Y. Deng, B. Tu and D. Zhao, *Angew. Chem. Int. Ed.*, 2010, **49**, 7987-7991.
8. Y. Fang, G. Zheng, J. Yang, H. Tang, Y. Zhang, B. Kong, Y. Lv, C. Xu, A. M. Asiri, J. Zi, F. Zhang and D. Zhao, *Angew. Chem. Int. Ed.*, 2014, **126**, 5470-5474.
9. J. Liu, S. Z. Qiao, J. S. Chen, X. W. Lou, X. Xing and G. Q. Lu, *Chem. Commun.*, 2011, **47**, 12578-12591.
10. Z.-A. Qiao, B. Guo, A. J. Binder, J. Chen, G. M. Veith and S. Dai, *Nano Lett.*, 2012, **13**, 207-212.
11. G.-H. Wang, J. Hilgert, F. H. Richter, F. Wang, H.-J. Bongard, B. Spliethoff, C. Weidenthaler and F. Schüth, *Nature Mater.*, 2014, **13**, 293-300.
12. Y. Wang, K. Wang, R. Zhang, X. Liu, X. Yan, J. Wang, E. Wagner and R. Huang, *ACS Nano*, 2014, **8**, 7870-7879.
13. G. Zheng, S. W. Lee, Z. Liang, H.-W. Lee, K. Yan, H. Yao, H. Wang, W. Li, S. Chu and Y. Cui, *Nature Nanotech*, 2014, **9**, 618-623.
14. W. Zhou, X. Xiao, M. Cai and L. Yang, *Nano Lett.*, 2014, **14**, 5250-5256.

15. J. Liu, S. Z. Qiao, S. Budi Hartono and G. Q. Lu, *Angew. Chem. Int. Ed.*, 2010, **49**, 4981-4985.
16. J. Liu, T. Yang, D.-W. Wang, G. Q. Lu, D. Zhao and S. Z. Qiao, *Nature Commun*, 2013, **4**, 2798.
17. T. Yang, J. Liu, Y. Zheng, M. J. Monteiro and S. Z. Qiao, *Chem. Eur. J.*, 2013, **19**, 6942-6945.
18. J. Tang, J. Liu, C. Li, Y. Li, M. O. Tade, S. Dai and Y. Yamauchi, *Angew. Chem. Int. Ed.*, 2014, **53**, DOI: 10.1002/anie.201407629.
19. N. Li, Q. Zhang, J. Liu, J. Joo, A. Lee, Y. Gan and Y. Yin, *Chem. Commun.*, 2013, **49**, 5135-5137.
20. T. Yang, J. Liu, R. Zhou, Z. Chen, H. Xu, S. Z. Qiao and M. J. Monteiro, *J. Mater. Chem. A*, 2014, **2**, 18139-18146.
21. N.P. Wickramaratne, J. Xu, M. Wang, L. Zhu, L. Dai and M. Jaroniec, *Chem. Mater.* 2014, **26**, 2820-2828.

TOC

